Electronic Supplementary Information for:

A POM-encapsulating 3D Porous Metal-organic Pseudo-*rotaxane* Framework

Hai-jun Pang,[a] Jun Peng,*[a] Chun-jing Zhang,[a] Yang-guang Li,[a] Peng-peng Zhang,[a] Hui-yuan Ma,[b] and Zhong-min Su*[a]

Table of the contents:

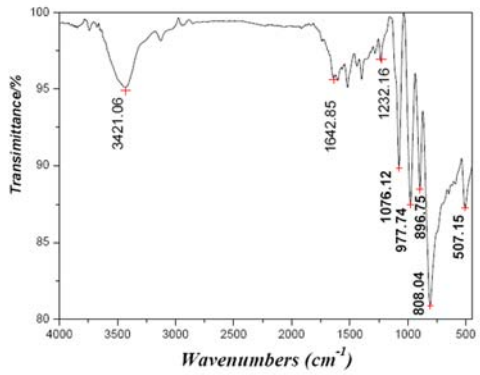

Fig. S1 IR spectrum of **1**.

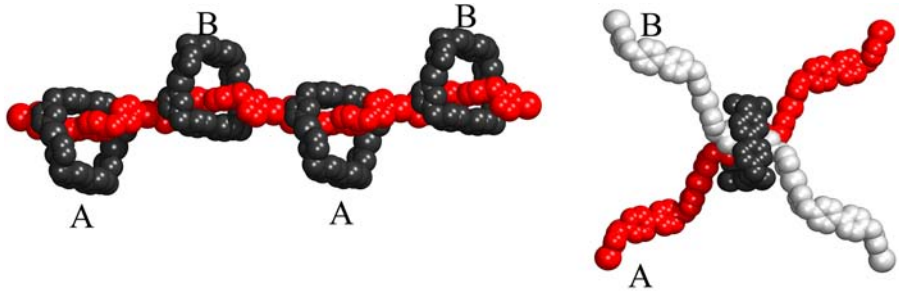

Fig. S2 A space-filling model showing the arrangement of molecular "loops" intercalated by one molecular ''string'' (left), and the unusual intercalated fashion of two ''strings'' in one "loops" (right).

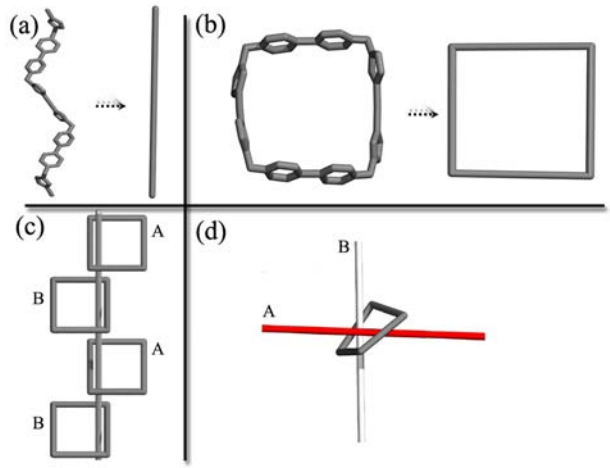

Fig. S3 A schematic presentation of the molecular ''string'' (a), molecular ''string'' (b), the arrangement of molecular "loops" intercalated by one molecular ''string'' (c), and the unusual intercalated fashion of two ''strings'' in one "loop" (d).

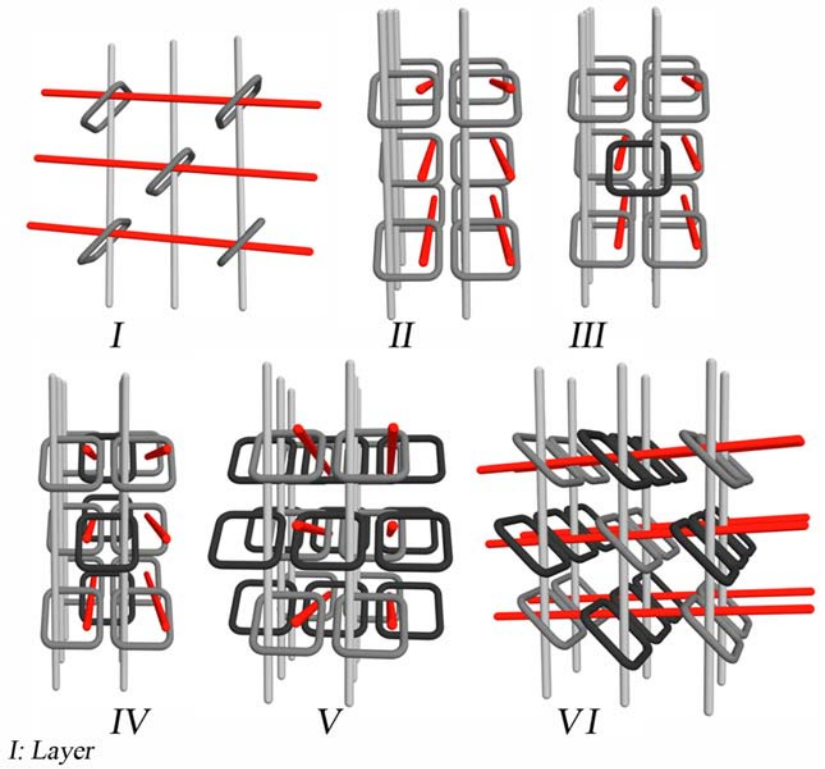

I: Layer

II: Two indie layers

III , IV and V: Schematic illustration of the entangled fashion of two layers

VI: after rotating the Figure V

Fig. S4 A schematic illustration of detailed entangled fashion in the MO*R*F.

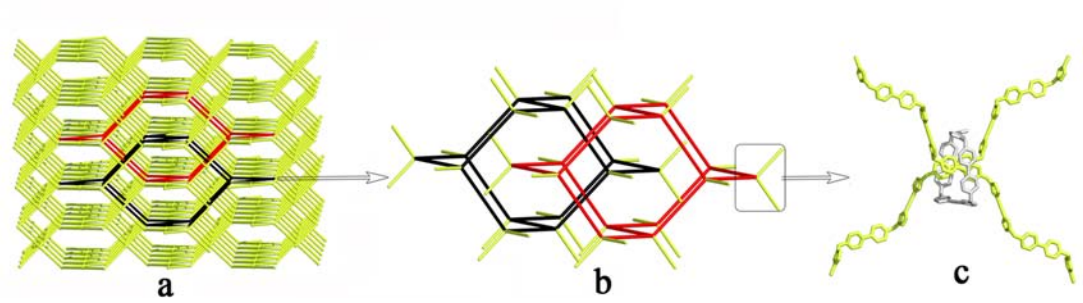

Fig. S5 Schematic view of the topology of 3D MO*R*F: 2-fold interpenetrated **dia** nets of Class Ia related by a single translation (a), the enlarged view of the interpenetration mode (b) and the entanglement of the two ‘‘strings’’ in one “loops” to shrink to a 4-connected node of the **dia** net (c).

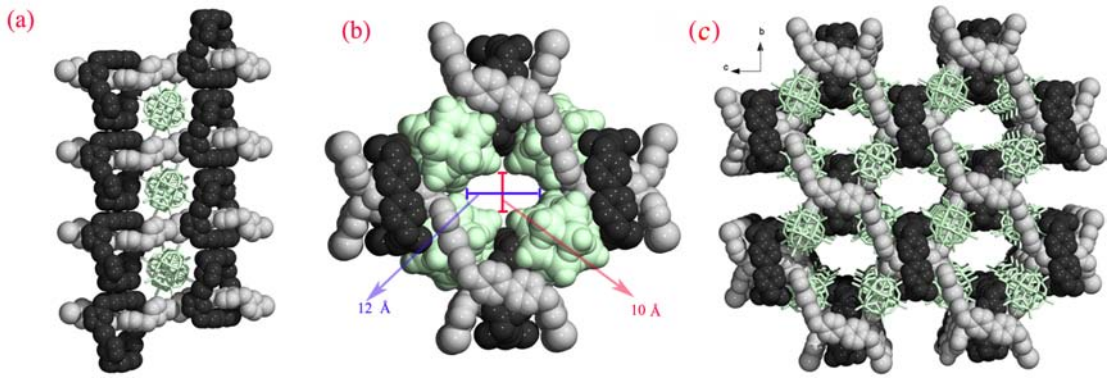

Fig. S6 A space-filling model showing the arrangement of the $[PW_{12}O_{40}]^{3-}$ clusters in the tunnels B/C (a) and A (b); View of the 1D tunnels along [011] direction (c). Guest water molecules are omitted for clarity.

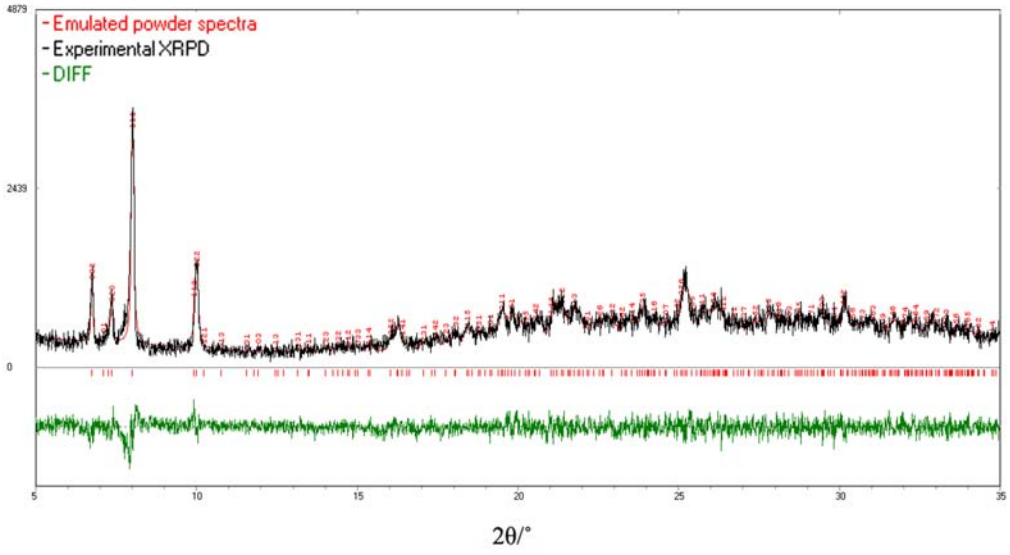

Fig. S7 Output of a calculated X-ray powder patterns by *POWDER CELL*.

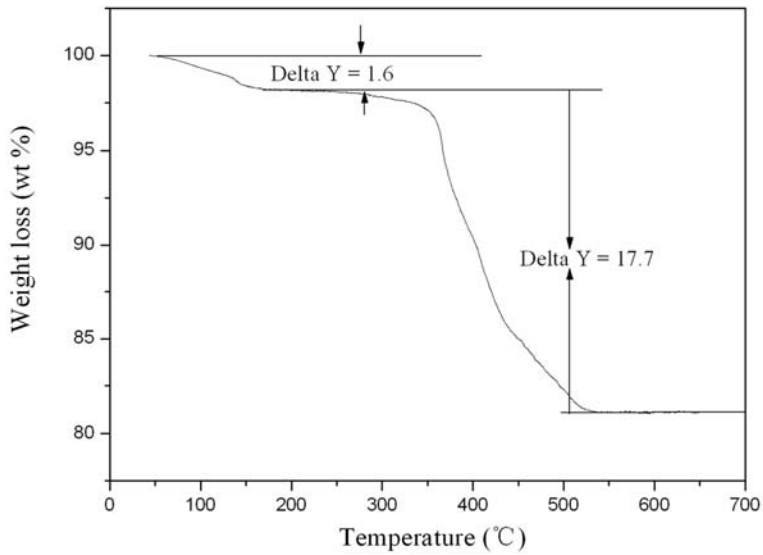

Fig. S8 TG curve of **1**.

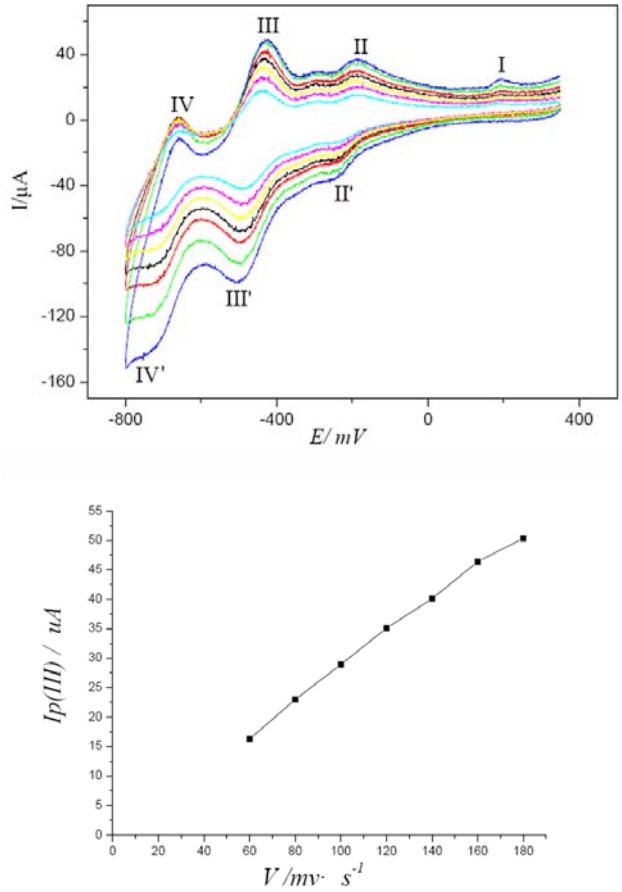

Fig. S9 Cyclic voltammograms of the **1-CPE** vs Ag/AgCl obtained at different scan rates (from in**n**er to outer: 60, 80, 100, 120, 140, 160, and 180 $mV \cdot s^{-1}$) in the 1 M H_2SO_4 solution (up) and the dependence of anodic peak current of III on scan rates (low).

Discussion

1 Structural feature of compound 1.

Polypseudo-*rotaxane* is a particular species of entangle system with the character that the "loops" are threaded by "strings", in which there are no hopf-links, no closed circuits are linked to other closed circuits.[1] The compounds with polypseudo-*rotaxane* structures have attracted more and more attentions due to their attractive structural features and potential applications. For example, Loeb et al. reported the first examples of charge neutral, metal organic polypseudo-*rotaxane* frameworks (MO*R*Fs) which were synthesized by the combination of a disulfonated-dibenzo-24crown-8 ether wheel and a dicationic 1,2-bis(pyridinium)ethane axle.[2] By introducing the flexible btx ligand into the molybdate system under the hydrothermal conditions, Xu and Dong obtained two compounds, $[Ag(btx)]_4[SiMo_{12}O_{40}]\cdot 2H_2O$ and $[Cu(btx)]_4[SiMo_{12}O_{40}]$, which respectively showed 0D + 1D and 1D + 2D polypseudo-*rotaxane* motifs.[3] We isolated the first polypseudo-rotaxane structure based on the Wells-Dawson polyoxometalate.[4] Very rencently, Stoddart and coworkers have constructed polypseudo-*rotaxanes* by choosing diverse mechanically bonded macromolecules and well discussed them in a tutorial review.[5]

In comparison with the examples mentioned above, compound **1** has three structure features. (a) The entangled fashion: in compound **1**, one ''loop'' encircles two ''strings'' rather than the common single one. (b) The unique POM-encapsulated porous MO*R*F structure: Compound **1** represents the first example of POM-encapsulated MO*R*F with well-defined 1D nano-scale tunnels bringing together the structure features of POMs, *rotaxanes* and PCPs. (c) The high dimension structure: usually, the dimension of the MO*R*F structures are 1D or 2D, whereas compound **1** possesses the 3D MO*R*F structure with a surprised topology of 2-fold 6^6 **dia** nets of the Class Ia.[6]

The topological analysis of the MO*R*F has been performed by reducing the entanglement of the two ''strings'' in one "loops" illustrated in Fig. S2, right, to a 4-connected node, that is, shrinking the macrocycle/loop to a point, resulting in a node

with 4 arms/strings pointing out in 4 directions. Surprisingly, the analysis of the topology of MO*R*F, according to a recent classification,[6] reveals that it belongs to Class Ia (the two identical interpenetrated 6^6 **dia** nets are generated only by translation and the translating vector is [100] (14.17 A)) (Fig. S5)".

2 Analyses of BVS, IR and TG measurements.

In compound **1**, all W atoms are in +VI oxidation state obtained by bond valence sum (BVS) calculations.[7] The copper atoms are all in +I oxidation state, confirmed by coordination environments, BVS calculations, and red color of the crystalline. The oxidation state of Cu center was changed from +II to +I in the preparation process, which is often observed in the hydrothermal reaction systems containing both N-donor of organic ligands and Cu^{II} ions.[8] Since **1** was isolated from acidic aqueous solution, one proton is attached to PW_{12} cluster to compensate charge balance, which is similar to the case of $[Ag_2(3atrz)_2]_2[(HPMo^{VI}_{10}Mo^{V}_{2}O_{40})]$.[9]

In the IR spectrum (see Fig. S1), the peaks at of at 808, 896, 981 and 1078 cm^{-1} are attributed to $\nu(P–O_c)$, $\nu(W=O_t$, $\nu_{as}(W–O_b–W)$ and $\nu_{as}(W–O_c–W)$ vibrations of α-Keggin cluster, respectively. The bands at 1231–1643 cm^{-1} region are assigned to characteristic peaks of the bimb lignds. Additionally, the band at 3428 cm^{-1} is ascribed to characteristic peak for water molecules.

The TG curve of **1**, which was performed in air to explore its thermal stability, exhibits two weight loss steps (Fig. S8). The first weight loss step of 1.6% (calc. 1.47%) below 250 °C corresponds to the loss of water molecules. The second weight loss step of 17.7% (calc. 18.76%) occurred in the range of 250–533 °C is ascribed to the decomposition of organic bimb molecules and collapse of Keggin PW_{12} clusters. The total weight loss is 19.3%, in consistence with the calculated value of 20.2% and also supporting the chemical composition of **1**.

3 The CVs of 1-CPE.

The CVs of **1**-CPE show three reversible redox processes in the potential range -800 to 400 mV. The mid-point potentials, $E_{1/2} = (E_{pa}+E_{pc})/2$, for the three processes are -216, -467 and -691 mV, respectively. The reduction processes (II' and III')

correspond to two consecutive one-electron reduction of W centers, while IV' corresponds to a two-electron process.[10] On the reverse scan, the irreversible anodic peak I observed at the peak potential of 186 mV is assigned to the oxidation of copper (I).[11] The linear dependence of anodic peak current of III on scan rates indicates possible surface-controlled process.

Reference

1. L. Carlucci, G. Ciani and D. M. Proserpio, *Coord. Chem. Rev.* 2003, **246**, 247.
2. L. K. Knight, V. N. Vukotic, E. Viljoen, C. B. Caputo and S. J. Loeb, *Chem. Commun.*, 2009, 5585.
3. B. X. Dong and Q. Xu, *Cryst. Growth Des.* 2009, **9**, 2776.
4. P. P. Zhang, A. X. Tian, J. Peng, H. J. Pang, J. Q. Sha, Y. Chen, M. Zhu and Y. H. Wang, *Inorg. Chem. Commun*., 2009, **12**, 902.
5. L. Fang, M. A. Olson, D. Benitez, E. Tkatchouk, W. A. Goddard III and J. F. Stoddart, *Chem. Soc. Rev.*, 2010, **39**, 17.
6. M. O'Keeffe, M. A. Peskov, S. J. Ramsden and O. M. Yaghi, *Acc. Chem. Res.*, 2008, **41**, 1782.
7. I. D. Brown and D. Altermatt, *Acta Crystallogr., Sect. B: Struct. Sci.*, 1985, **41**, 244.
8. C. M. Liu, D. Q. Zhang and D. B. Zhu, *Cryst. Growth Des.* 2005, **5**, 1639.
9. Q. G. Zhai, X. Y. Wu, S. M. Chen, Z. G. Zhao and C. Z. Lu, *Inorg. Chem.* 2007, **46**, 5046.
10. M. T. Pope and G. M. Varga, *Inorg. Chem*. 1966, **5**, 1249.
11. A.-X. Tian, J. Ying, J. Peng, J.-Q. Sha, Z.-G. Han, J.-F. Ma, Z.-M. Su, N.-H. Hu and H.-Q. Jia, *Inorg. Chem.* 2008, **47**, 3274.